Solar Energy 263 (2023) 111954

Contents lists available at ScienceDirect

Solar Energy

journal homepage: www.elsevier.com/locate/solener

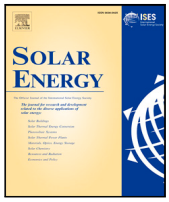

The cost-saving potential of next-generation particle technology CSP with steam cycles

Lukas Heller [a,*], Dennis Többen [b], Tobias Hirsch [a], Reiner Buck [a]

[a] German Aerospace Center (DLR), Institute of Solar Research, Stuttgart, Germany
[b] MAN Energy Solutions, Oberhausen, Germany

ARTICLE INFO

Keywords:
Particle technology
CSP
Techno-economic optimization
CentRec

ABSTRACT

The cost-saving potential of next-generation concentrating solar power plants based on particle technology with steam cycles is assessed. Techno-economic models were created to optimize three systems with different steam cycles, ranging from state of the art to future development, for levelized cost of electricity and to compare them to a state-of-the-art molten salt tower system. Results show that the minimum levelized cost for a particle system is almost identical to that of a molten salt system (+ 0.1 %), however larger solar multiples and storage capacities are preferred. Cost advantages for the receiver and storage subsystems are compensated for by increased costs for a multi-tower setup and the particle heat exchanger. The choice of the three investigated power cycles has only a marginal impact on the overall levelized cost (< 2.3 %). Finally, several potential improvements to particle systems are identified which could lead to further cost reductions and an increase in electric yield.

1. Introduction

It is generally agreed on, that future electricity generation has to come predominantly from renewable energy sources. Compared with other technologies that allow for a large increase in deployment, i.e. wind power and photovoltaics, concentrating solar power (CSP) can be equipped with a cost-effective multi-hour thermal energy storage. It is, therefore, not a fluctuating source to an electric grid but can offer dispatchable power on demand.

In order to further improve CSP plants' cost competitiveness compared with alternative electricity generation technologies, for example fluctuating renewables plus electric batteries, the levelized cost of electricity (LCOE) needs to be reduced. Next-generation CSP technologies aim at increasing the solar-to-electric efficiency and lowering the overall investment and operational cost. Using solid particles as the heat transfer medium (HTM) has the potential to achieve this in multiple ways:

- Particles can be irradiated directly by concentrated solar radiation without the need for additional absorbing and conducting materials. This can lower the cost of the receiver system, increase its efficiency and alleviate temperature restrictions.
- The upper operating temperature limit of the particles lies above 1000 °C, meaning that higher-efficiency steam or supercritical CO_2 (sCO_2) power cycles can be employed. Furthermore, large approach temperatures in HTM heat exchangers are feasible which can lead to lower heat transfer surface area requirements.
- The lower operating temperature limit of the particles lies far below 0 °C. This makes heat tracing obsolete, which is needed in molten salt plants to keep the HTM liquid at all times. Hence, the HTM loop is simplified and operation and maintenance (O&M) costs as well as parasitic energy consumption lowered.
- A large temperature spread between hot and cold storage tank is possible, which allows for smaller storage volumes and lower cost.
- Transport of particles over intermediate distances is conceivable due to the higher storage density and the lack of a need for freezing protection. This could allow for the utilization of CSP at locations that were formerly thought to be unsuitable.
- There is thorough knowledge in industrial manufacturing of suitable particles as these are used in very large quantities by the fracking and casting industry. It is expected that they can be manufactured almost entirely from recycled material [1] and they are environmentally benign.

While there is, thus, a great cost-saving potential in particle technology, there are also considerable technological risks and economic

* Corresponding author.
E-mail address: Lukas_Heller@gmx.de (L. Heller).

https://doi.org/10.1016/j.solener.2023.111954
Received 15 March 2023; Received in revised form 5 July 2023; Accepted 15 August 2023
Available online 1 September 2023

Nomenclature

Variables

C	Cost (USD)
h	Heat transfer coefficient $\left(\mathrm{W/(m^2\,K)}\right)$
$LCOE$	Levelized cost of electricity $\left(\mathrm{USD/(kW_e\,h)}\right)$
SM	Solar multiple (−)
UA	Heat exchanger conductance-area product (W/K)
η	Efficiency (%)

Subscripts

e	Electrical
t	Thermal

Abbreviations

CSP	Concentrating solar power
EPC	Engineering, procurement and construction
HTM	Heat transfer medium
LCOE	Levelized cost of electricity
O&M	Operation and maintenance
PHX	Primary heat exchanger
sCO_2	Supercritical carbon dioxide
TES	Thermal energy storage
TIT	Turbine inlet temperature

uncertainties. All particle-related components remain to be demonstrated at realistic operating conditions and scale. Most importantly, this concerns the receiver, heat exchanger, transport and thermal energy storage systems. Furthermore, state-of-the-art power cycles at the typical size of utility-scale CSP plants ($\approx 100\,\mathrm{MW_e}$ to $150\,\mathrm{MW_e}$) operate at a turbine inlet temperature, TIT, of approximately 550 °C. To take full advantage of the higher achievable temperature of particle technology, new developments in power cycles are also needed (using steam or sCO_2 as the working fluid).

In the KOSTPAR Project (funded by the German Federal Ministry for Economic Affairs and Climate Action), partners from industry (Steinmüller Engineering, MAN Energy Solutions SE and ROBA Piping Projects GmbH) and Research (DLR and Forschungszentrum Jülich GmbH) aimed at elevating these components to higher technology readiness levels and assessed the techno-economic performance of a utility-scale particle CSP plant with advanced steam power cycles. This study concerns this latter assessment, the direct comparison of a particle-based system with state-of-the art molten salt plants.

Particle technologies are currently being investigated in several research and development projects [e.g. 2–4] and the technology has been identified as one of the most promising candidates for bringing down cost in next-generation installations [5]. In a few studies, the techno-economic potential of particle CSP power plants has been evaluated in terms of levelized cost of electricity (LCOE).

Albrecht et al. [6] developed a coupled model of a particle CSP system with a sCO_2 power block. They used the model to investigate the effect of power block operating parameters and particle material properties on the overall LCOE. They found that particle-sCO_2 plants could achieve the ambitious goal set out by the United States Department of Energy of $6\,\mathrm{USD\text{-}cent/kW_e h}$. However, their models used aggressive cost targets instead of vendor quotes for some of the major subsystems and components (e.g., power block, primary heat exchanger (PHX) and heliostat field). The resulting LCOE values are, hence, not comparable to reference values of molten salt systems.

González-Portillo et al. [7,8] upgraded the model by Albrecht et al. [6], adding off-design capabilities and improvements to several component models (especially of the receiver and particle lift). Furthermore, cost models were updated and the sensitivity of the LCOE on changes in component costs was investigated. However, the costs of power block, PHX and heliostat field were not changed. That model was not used to simulate a reference molten salt system but a reference cost for such system was derived from another model. The calculated particle system costs were found to be significantly lower than that reference cost.

Similarly, Buck and Giuliano [9,10] as well as Buck and Sment [11] assessed the techno-economics of particle technology-based CSP systems. The concepts they modeled are designed around a different type of particle receiver, the CentRec®, which allows for greater flexibility in operating temperatures. They studied the economic benefits of different hot and cold tank temperatures and found that a high temperature spread, i.e. a high hot tank temperature and a rather low cold tank temperature, render the lowest LCOE. While two of the studies looked at sCO_2 power cycles, Buck and Giuliano [10] assumed an advanced steam cycle (with a TIT of 620 °C). The specific cost of the particle thermal storage system was found to be approximately half of the one of a molten salt power tower, however, the costs of the remaining subsystems or the total cost were not compared.

Heller et al. [12] developed a simplified techno-economic model to pre-select sCO_2 power cycles with a high potential to lower the LCOE of next-generation CSP plants. For the investigated sCO_2 cycles, they found significantly lower LCOE values for particle systems, featuring CentRec® receivers, than for reference molten salt towers. Mainly the TES and the receiver subsystems were cheaper compared with the reference, while the towers and HTM transport systems had higher capital cost. These results, however, are not transferable to CSP plants with steam cycles, as the temperature spread in the PHX of the investigated sCO_2 cycles is much smaller than typical for steam cycles, leading to a higher TES cost. Furthermore, the used cost model for the molten salt receiver system is based on old sources and quite conservative compared with recent studies [13].

In an earlier study, Ma et al. [14] proposed a different particle CSP technology featuring a closed receiver system and a fluidized bed heat exchanger to run high-efficiency power cycles. They estimate that a plant of this concept will generate electricity at 20 % lower LCOE values than molten salt tower systems, however, no details on the modeling approach or the source of the cost data was presented. The cost shares, for which the biggest advantage over the state of the art is given, are the storage system, the tower/receiver system and O&M cost.

It can be concluded that, although there is a small number of techno-economic assessments of next-generation particle CSP systems, there is a clear lack of a direct simulation comparison of such systems with a state-of-the-art molten salt tower system. This comparison, however, is deemed to be of great significance in order to fairly quantify the expected economic advantages of particle CSP technology.

In the present study, the cost-saving potential of next-generation CSP plants based on CentRec® particle technology is assessed through a detailed techno-economic analysis and the comparison to a state-of-the-art plant utilizing molten salt as the HTM. An energetic model of the setup is developed from performance data provided by partners in research projects and from estimates for some less-developed components. As the costs of most particle-related subsystems have a large uncertainty, the optimization and comparison was repeated with different cost models for the particle heat exchanger. Finally, several technological improvements that could result in further cost reductions of particle systems are presented.

2. Modeling and simulations

In this section the assessed particle CSP plant concept, details on the technical and economic modeling as well as the optimization approach are presented. Furthermore, the molten salt reference system model is defined.

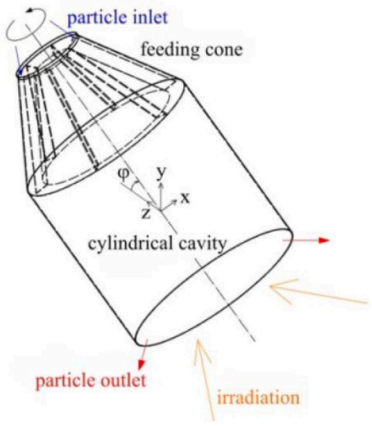

Fig. 1. CentRec® concept [15].

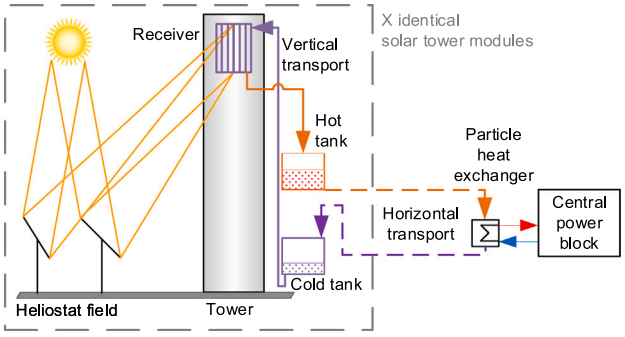

Fig. 2. Schematic of the solar particle loop [12].

2.1. Plant concept

The solar collector system of the modeled particle technology plants is of the multi-tower type. On top of each tower, a single CentRec® receiver with a design-point rating of 40.4 MW_t is installed. These particle receivers feature a rotating drum with a circular aperture opening (see Fig. 1), forming a cavity and requiring a polar field layout. The practical size limitation of polar fields, due to the large distance of additional heliostats, requires the chosen multi-tower layout for utility-scale CentRec® technology power generation plants. The thermal energy storage (TES) system in the plant is foreseen to be decentralized, i.e. each tower houses its own set of hot and cold particle tanks and a vertical particle transport system to the receiver inlet (see Fig. 2). Several of these identical collector systems are located in proximity to a central power block with particle PHX. The horizontal transport of particles between towers and central power block is foreseen in insulated standard shipping containers by means of autonomous vehicles [11].

2.2. Thermodynamic models

Thermodynamic models of all subsystems were developed based on input from industrial partners in the KOSTPAR project and on performance estimates of those components for which no applicable data was available. These models are described in the following sections. Numeric values for all important parameters are presented in a comprehensive data book in Appendix B.

2.2.1. Capacity, location and solar field

The capacity of the modeled power plant (100 $MW_{e,net}$) and its location (Ouarzazate, Morocco) are representative of a typical solar tower plant.

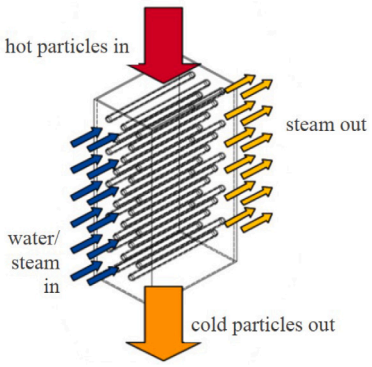

Fig. 3. Schematic of the particle steam generator (from Buck and Giuliano [10], based on Baumann and Zunft [19]).

The solar receiver is based on the CentRec® technology [15]. The receiver outlet temperature was fixed at 900 °C as this has been demonstrated for the technology [16], although higher values promise even better economic performance [9]. The receiver's thermo-optical efficiency was calculated with a correlation that was derived from limited test data and numerical simulations [see 9,17].

The tool Visual HFLCAL [18] was used to optimize the number of heliostats, their location, the receiver aperture area and tower height for minimized levelized cost. For each of the tower modules the identical solar field layout was chosen. The number of modules, representing the solar multiple, was varied in a sensitivity analysis (see Section 3).

2.2.2. Power block and PHX

Three different steam power cycles were modeled by the project partner MAN Energy Solutions SE. The first configuration is a standard, non-reheat steam cycle with moderate live steam parameters (540 °C, 140 bar). The second configuration represents a state-of-the-art subcritical steam cycle featuring a single re-heating stage and more demanding parameters (565 °C, 160 bar), requiring high-cost materials for certain components. The final configuration additionally features a re-heating stage and live steam parameters (620 °C, 180 bar) requiring expensive, high-performance alloys. While these materials are generally known and have been tested in supercritical steam cycles, further developments are needed before these specific processes can be used in commercial power plants at the intended power level.

Steinmüller Engineering compared two different concepts for the particle steam generator, namely a fluidized-bed and a moving-bed design. The former was not followed due to high expected approach temperatures between steam inlet and particle outlet, technological challenges (e.g., erosion) and high cost for a commercial design. It was, furthermore, decided to use horizontally oriented plain tubes (see Fig. 3) and to fix the approach temperature to 150 K. This latter value was later reevaluated (see Section 3.4).

Due to limited available data, no distinction was made between the pressure drop of the three PHX variants. For the same reason, the energy demand for starting up the PHX and power block were neglected. Due to the similarity of all power block variants, this is expected to have only a marginal impact on the comparison in between them and close to no impact on the comparison of the reference system with a particle system with identical power cycle.

2.2.3. TES & transport systems

Each tower houses two tanks (for hot and cold particles, respectively) and a vertical transport system. Thermal losses from the TES system and from the ground transport system (incl. filling processes) are estimated as 1 % of the maximum storage capacity per day and 2 % (round-trip) of the transported energy, respectively. The parasitic energy consumption to lift cold particles to the receiver and to lift

hot particles above the central PHX is calculated based on estimated efficiencies. The consumption for ground transport is estimated to be in the order of 0.1 % of the generated electricity and has, therefore, been neglected due to uncertainties surrounding the used transport technology. The cold tank particle temperature (400 °C) is the same for each of the three power block variants as their feed-water temperature as well as their PHX approach temperatures are identical.

2.2.4. Annual yield calculation

A tool chain of the software suits HFLCAL, Ebsilon Professional v. 14.03 and Microsoft Excel is used to calculate each variant's annual electric yield. The hourly heat input to the particle loop is calculated in Excel from meteorological data, an efficiency matrix of the solar field (generated in HFLCAL), the receiver efficiency correlation and operating limits of the receiver. Depending on the remaining thermal energy in the TES, an Ebsilon model of the power block and the PHX is activated in a specific operating mode and the electric yield is calculated under the current boundary conditions (i.e., available input to the PHX and ambient temperature). In order to make the results comparable for different applications, the operating strategy was set to generate electricity whenever possible (as opposed to, e.g., a peaker plant).

2.2.5. Reference molten salt system

An equivalent annual yield model was developed for the molten salt reference configurations. To make the comparison with particle systems as fair as possible, it was attempted to keep most boundary conditions and assumptions identical unless there was well-founded reason to deviate. In the following, only these deviations are described.

Current molten salt tower systems operate at HTM temperatures below 565 °C to avoid fluid degradation and excessive corrosion [13]. Of the three modeled steam processes, only the simplest variant could be utilized under this boundary condition. This differs from state-of-the art plants, in which processes with at least one re-heat stage and a potentially slightly higher TIT than 540 °C are used to boost efficiency [13]. However, it was observed that the non-reheat process investigated in this study reaches a remarkably high thermal efficiency of 41.4 %. This compares favorably with a more advanced process, recently designed by MAN Energy Solutions [13] for molten salt plants, which reaches 41.5 %. As the difference in performance is small, it was decided to use the 540 °C process for the molten salt reference system. This decision is further justified as the difference in LCOE between particle plants using each of the three power block processes was found to be small (see Section 3.2).

Contrary to the assessed particle technology, commercial molten salt systems have single-tower solar fields. At first, a single reference system with a fixed solar field size and storage capacity was used. As the techno-economic optimum for the particle systems was found to be at much larger values for these two parameters, they were also varied for the reference system. Due to the non-modular solar field, this required individual field optimizations in HFLCAL for each solar multiple variation.

Furthermore, estimates for several parameters in the HTM loop differ between the two technologies. Most noticeably, this concerns the energy requirement for receiver start-up and parasitics for HTM transport (salt pumps vs. particle lifts). The numeric values for these parameters applicable to either of the two models are compiled in Appendix B.

2.3. Economic models

Due to the novelty and low maturity of solar particle technology, for most components no commercial cost data could be found in literature. Hence, most of the developed cost models rely on estimates by DLR and from a joint study with Sandia National Laboratories [11]. The used specific cost correlations and economic parameters are listed in Table 1 and elaborated on in this section. As all sources of cost data were published in close temporal proximity (years 2019–2022) and because of the extraordinary price developments and exchange rate fluctuation since 2020, these data were not adjusted for inflation.

The direct cost for the EPC (engineering, procurement and construction) contractor is the sum of the subsystem costs

$$C_{\mathrm{EPC,direct}} = C_{\mathrm{HelioF}} + C_{\mathrm{Land}} + C_{\mathrm{Towers}} + C_{\mathrm{Rec}} + C_{\mathrm{TES\&HTM}} + C_{\mathrm{transpT}} + C_{\mathrm{transpPHX}} + C_{\mathrm{transpH}} + C_{\mathrm{BoP}} + C_{\mathrm{PHX}} + C_{\mathrm{PB}}. \quad (1)$$

Therein, the costs for heliostat field, land, towers and receivers (C_{HelioF}, C_{Land}, C_{Towers} and C_{Rec}) are based on literature or DLR-internal estimates for specific costs, as given in Table 1. Likewise, costs for vertical transport systems in the towers (C_{transpT}) and at the PHX ($C_{\mathrm{transpPHX}}$) were derived from a study by Sandia National Laboratories [6]. The correlations for the costs of the horizontal transport system (C_{transpH}) and the TES system including particle inventory ($C_{\mathrm{TES\&HTM}}$) were derived from a joint study by authors from both of these institutions [11] and are described in detail in Appendix A. The costs for power block and balance of plant (C_{PB} and C_{BoP}) were defined by MAN Energy Solutions.

A literature study revealed that cost models for particle PHXs are not in good agreement. The costs as calculated with the identified models for a range of area-conductance products, $(UA)_{\mathrm{PHX}}$, are depicted in Fig. 4. While they were not developed for identical conditions (working fluid, temperatures, pressures, heat exchanger technology), the range of resulting costs indicates a high level of uncertainty, caused by the lack of real-world demonstrators of the technology. For the present model, it was decided to use an upper and a lower boundary correlation for the PHX cost (dashed orange lines in Fig. 4), as proposed by Buck and Sment [11], to calculate a range of likely results.

These correlations, with the exception of the one by Buck and Giuliano, were developed for a particle-to-sCO_2 plate heat exchanger and are, therefore, not directly transferable to the tubular designs for steam generation proposed in this study. While the former technology is predicted to enable superior heat transfer compared to more conventional designs, it can currently only be manufactured in limited geometrical sizes. A utility-scale design would, therefore, comprise of several parallel units with extensive particle and fluid distribution systems. As a conservative approach, the cost models of the plate heat exchanger were used for the tubular heat exchanger but the heat transfer coefficient (h_{PHX}) was lowered from 496 W/(m^2 K) to 300 W/(m^2 K) [compare with 9,20]. Assuming that the overall thermal transmittance is dominated by this heat transfer coefficient, the heat transfer surface area of the PHX (A_{PHX}), which is the determining parameter for its cost, is then calculated as

$$A_{\mathrm{PHX}} = (UA)_{\mathrm{PHX}} / h_{\mathrm{PHX}}. \quad (2)$$

It is worth noting, that this cost model does not consider the live steam temperature as a parameter and that the correlations were developed for sCO_2 with temperatures of up to 700 °C. For the assessed steam processes, especially the lower-temperature ones, the correlations might therefore be conservative.

To calculate the overall project cost, $C_{\mathrm{overnight}}$, for each variant, the direct EPC cost is multiplied by a factor representing EPC services, profit and owner's cost:

$$C_{\mathrm{overnight}} = (1 + f_{\mathrm{EPC+owner}}) C_{\mathrm{EPC,direct}}. \quad (3)$$

The levelized cost is calculated in a simplified manner from this total cost, the fixed and variable annual cost for O&M ($C_{\mathrm{O\&M,a,fix}}$ and $C_{\mathrm{O\&M,a,var}}$, respectively), insurance cost (C_{insur}) and the annual electric yield, $E_{\mathrm{plant,net,a}}$:

$$LCOE = (FCR\, C_{\mathrm{overnight}} + C_{\mathrm{O\&M,a,fix}} + C_{\mathrm{O\&M,a,var}} + C_{\mathrm{insur}}) / E_{\mathrm{plant,net,a}}. \quad (4)$$

Therein, the fixed charge rate, FCR, is defined by the real discount rate, i, and the project lifetime, n:

$$FCR = i(1+i)^n / \left((1+i)^n - 1\right). \quad (5)$$

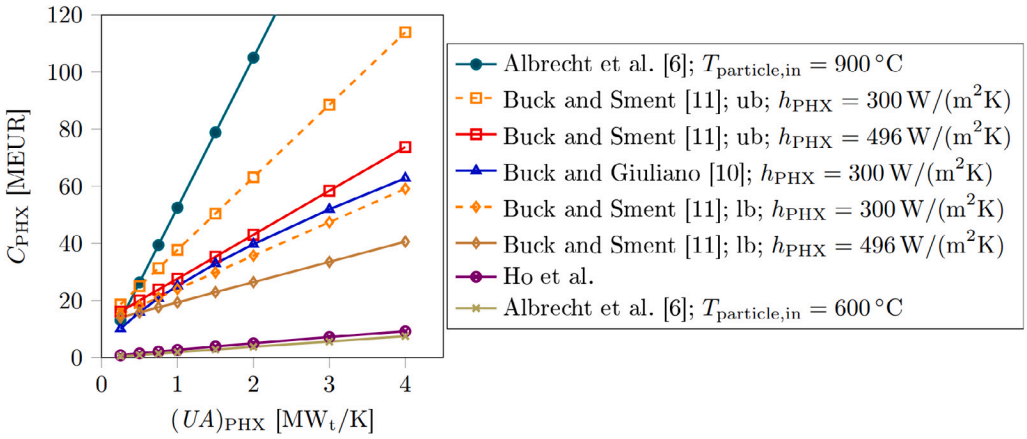

Fig. 4. PHX cost correlations from literature; where indicated, an overall heat transfer coefficient, h_{PHX}, was used in combination with Eq. (2) to calculate the UA value; ub: upper bound; lb: lower bound.

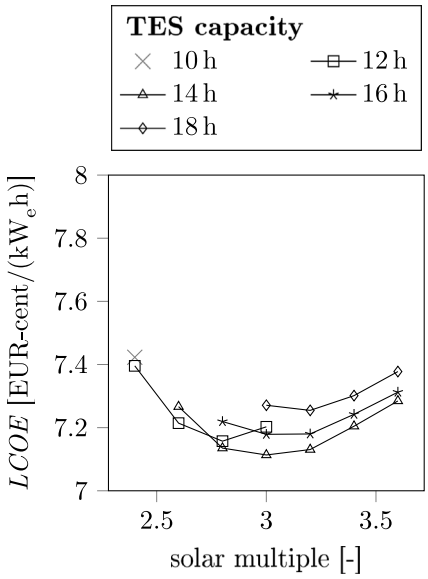

Fig. 5. Levelized cost of molten salt reference systems.

3. Results and discussion

For each of the four modeled HTM-power cycle combinations (i.e., the molten salt system and the particle system with each of the three power cycles), the solar multiple and storage capacity were varied to identify the configurations with the lowest LCOE. This was repeated for each of the two PHX cost models. In the following, the results of these optimizations are presented and compared. Subsequently, potential improvements to the particle systems are proposed.

3.1. Reference molten salt systems

Initially, it was planned to only simulate a single molten salt reference system with a solar multiple of 2.4 and a storage capacity of 10 h. However, it became apparent that systems with higher values for both of these parameters render lower LCOE values for molten salt (see Fig. 5) and for particle systems. For the following technology comparisons, only those molten salt configurations with the lowest LCOE at a given solar multiple are shown (pareto front).

3.2. Steam process variants

The three plots in Fig. 6 depict the levelized cost curves for the investigated power block variants as calculated using the lower bound correlation for the PHX cost. Three important observations can be made from the plots:

1. For every power block variant, the lowest LCOE of all particle systems is higher than the one of the molten salt reference system. The difference between the two HTM technologies is, however, rather small at +2.4 % to +0.1 % for a TIT of 540 °C and 620 °C, respectively. The comparison becomes most favorable for the particle variants, when high plant utilization is sought after (i.e., large storage capacity and high solar multiple).
2. The LCOE minima of particle systems are reached with configurations that feature a large solar multiple and storage capacity ($3 < SM_{opt} < 3.6$; $14\,h < Q_{TES,opt} < 20\,h$). The sensitivity for storage capacity is rather low, which is caused by low specific costs of the particle TES system (approximately 14 EUR/kW_th). Compared with the reference system, larger solar fields are more viable due to the linearly increasing costs and constant optical efficiency of multi-tower setups.
3. The difference in minimum LCOE of the three steam cycles is small (<2.3 %). The higher efficiency of the high-performance steam cycles appears to be almost compensated by their higher cost.

As none of the particle systems reaches a lower LCOE than the one of the reference system when using the lower bound cost correlations for the PHX, this is obviously also true when the higher bound correlation is used. For the sake of completeness, the results for configurations featuring the 565 °C process are presented in Fig. 7. The difference in calculated LCOE between the two cost models is rather small. Firstly, this is caused by a large share of fixed costs for PHX piping and manifolds (12.3 MEUR), which is identical in both cost correlations. Secondly, the share of PHX cost in total plant costs ($C_{EPC,direct}$) is only approximately 6 % and 9 % for the lower and upper boundary, respectively (see following section).

3.3. Detailed comparison of three configurations

A detailed performance and economic comparison was conducted for three selected configurations: A molten salt reference system (blue, solid bars in Fig. 8), a particle system with the identical power block (540 °C) and a similar annual power output ($E_{net,a}$) as the reference system (orange, striped) and the particle system with the lowest LCOE (green, dotted). The results indicate the following:

- The subsystem costs of the two particle configurations are very similar. Only the power block of the 620 °C configuration is visibly more expensive, however, the system also has a larger annual output.

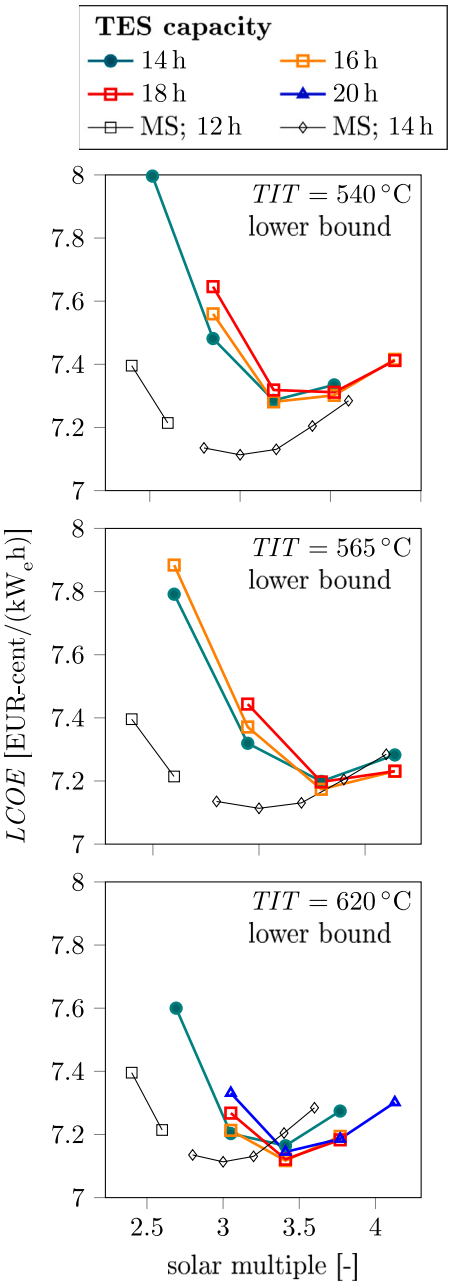

Fig. 6. Levelized cost of all configurations for each of the three steam processes, calculated using the *lower bound* cost correlation for the PHX; all MS configurations feature a TIT of 540 °C.

- The CentRec® receiver system is significantly more cost effective than the reference receiver system.
- The large number of towers in the particle configurations incur much higher costs than the single tower of the salt system.
- The particle TES system (including adjustments to the tower structure) is considerably cheaper than state-of-the-art molten salt technology. At an identical capacity, the savings are approximately 33 %.
- The particle PHX is predicted to cost more than twice as much as the molten salt design (even though the lower bound cost correlation was used).

Some design point parameters, subsystem annual efficiencies and cost figures of the comparison are provided in Table 2. One interesting observation from this data is that the design point efficiency of heliostat field and receiver subsystems is higher for the particle systems, while this is reversed for the annual values. This is not an unexpected behavior for polar heliostat fields, which tend to have higher peak efficiencies compared with surrounding fields. This phenomenon explains why larger solar multiples are needed in particle systems in order to achieve the same annual electrical yield, compared with the reference system.

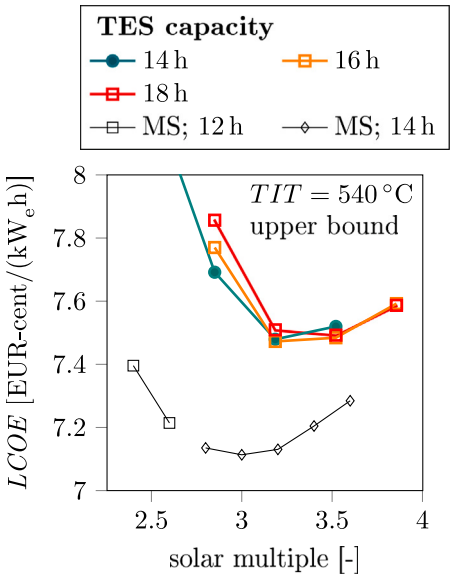

Fig. 7. Levelized cost of all configurations for the 540 °C steam process, calculated using the *upper bound* cost correlation for the PHX.

Furthermore, a higher ratio of plant net efficiency to power block net efficiency of the particle systems is apparent (approximately 99.3 % compared with 97.1 %). The main driver is the lower power consumption for vertical HTM transport in the towers (0.5 % compared with 2.6 % of plant gross power generation). Parasitic power consumption for molten salt receiver start-ups is less significant at 0.2 %.

3.4. Potential improvements to particle systems

Several possibilities exist to improve the techno-economic performance of particle technology CSP plants. These were not added to the previously described models due to their low technological maturity and uncertain costs. Some are, nevertheless, discussed here for the sake of completeness and, where preliminary (unpublished) assessments exist, an estimate on their potential benefit is given.

- The high solar fluxes (around 2.2 MW/m^2, compared with 600 kW/m^2 in the reference system), which are necessary to achieve a high thermal efficiency of the receiver at the present HTM outlet temperatures, cause optical (spillage) losses in the order of 15 %. If this lost energy can be utilized for power generation (e.g., via concentrating photovoltaic, CPV, cells around the receiver), significant annual electric yield improvements could be achieved. In the on-going SpiCoPV project [23], optimized systems were found to reach LCOE improvements of up to 10 % to 15 % at CPV-to-CSP annual electric yield fractions of approximately 20 % (assuming a CPV system efficiency of around 32 %).
- Only small improvements in levelized costs (≈1 %) are expected for setups in which several receivers are installed on a single tower, pointing in different directions (multi-eye). Combining this with switching the focus of certain heliostats to a different receiver (multi-focus) depending on the sun position could, however, lead to a significant increase in annual yield of up to 5 %.

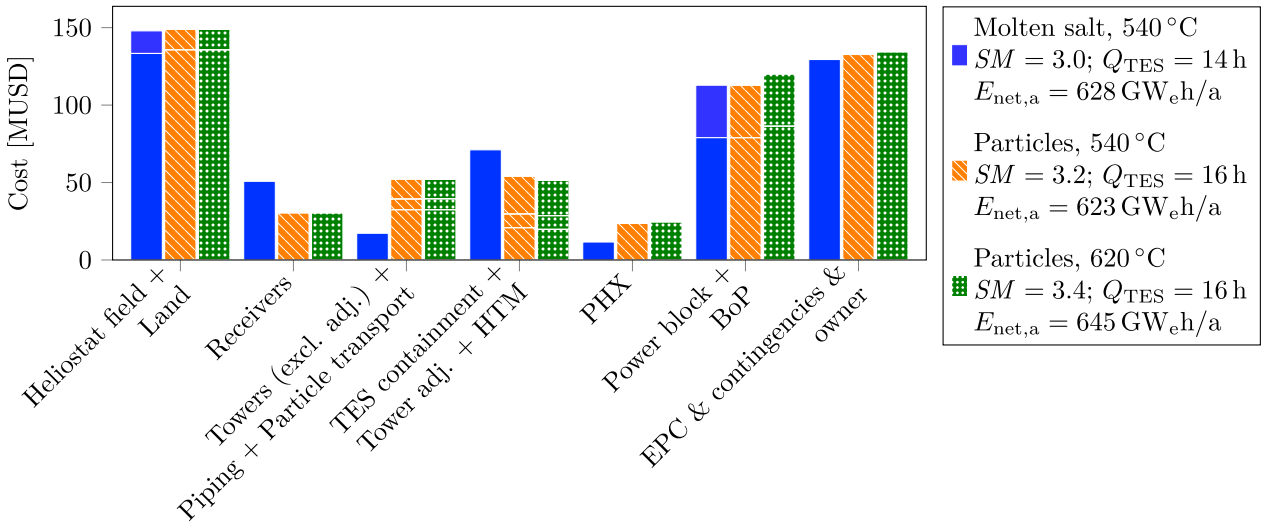

Fig. 8. Subsystem costs of three plant configurations: molten salt, particle technology with a comparable annual output and particle technology with the lowest LCOE, calculated using the *lower bound* cost correlation for the PHX (naming of the stacked bars from bottom to top); adj.: costs for adjustments in tower structure for TES integration.

Table 1
Cost correlations and economic parameters.

Subsystem/parameter	Unit	Molten salt	Particles	Comments
Heliostat field	[EUR/m^2]	100		[13]
Land	[EUR/m^2]	2		
Towers	[EUR]	$-731\,236 + 65\,204(H/\mathrm{m}) - 148.25(H/\mathrm{m})^2 + 0.7452(H/\mathrm{m})^3$	$742\,194 + 108.44(H/\mathrm{m})^{1.94} + 217.72(H/\mathrm{m})^{1.81}$	[21, p. 118] |[11] interpolated to 900 °C, incl. TES integration; H: optical height
Receiver	[EUR/kW$_t$]	70		[13] |
	[EUR/m^2]		80 000	|DLR estimate
Vert. transport	[EUR/(kg/s m)]	Incl. in receiver	49.26	|[6]
Horiz. transport	[−]		s. Appendix A	
TES	[EUR/kW$_t$h]	21	s. Appendix A	[13] |
Particles	[EUR/kg]		1.00	|[11]
PHX	[EUR/kW$_t$]	47.9		[13] |
Lower bound	[−]		12.27 MEUR + 3509 EUR/m^2 A_{PHX}	|[11]
Upper bound	[−]		12.27 MEUR + 7621 EUR/m^2 A_{PHX}	|[11]
Power block	[EUR/kW$_{e,gross}$]	750	750/787.5/825	TIT: 540 °C/565 °C/620 °C
Balance of plant	[EUR/kW$_{e,gross}$]	322		[13]
EPC, $f_{EPC+owner}$	[%]	31.4		see Eq. (3)
O&M variable	[EUR/MW$_{e,net}$h]	2.95		[22, Table 3]
O&M fix	[EUR/(kW$_{e,net}$a)]	55.7		[22, Table 3]
Insurance	[%/a]	0.5		[22, Table 3]
Life time	[a]	30		[11]
Real discount rate	[%/a]	5		
Exchange rate	[USD/EUR]	1.185		[11]

- A decrease in the cold tank temperature could lower TES and HTM transport system costs. Higher costs for the PHX, due to an increase in surface area, would have to be compensated, though. A limited sensitivity analysis, based on the presented cost models for PHXs, was conducted to estimate the cost saving potential (see Fig. 9). If the lower bound PHX cost correlation is used, a decrease in LCOE of less than 0.5 % was found when lowering the cold tank temperature from 400 °C to 300 °C. The latter corresponds to a terminal temperature difference of 50 K in the PHX. If the upper bound correlation is used, the most cost effective cold tank temperature is 400 °C. The changes in subsystem costs for both PHX cost correlation are shown in Fig. 10.
- An increase in the hot tank temperature, e.g. to 1000 °C, would have the same effect on TES and HTM transport system costs while also allowing for smaller PHX surface areas [10]. However, technical feasibility of increasing the receiver outlet temperature and economic repercussions of the higher system temperatures will have to be investigated.
- Since the integration of TES systems into every solar tower entails significant costs and potentially higher thermal losses, the design of central storage tanks should be assessed.
- Lower tower system costs through standardized on-site manufacturing techniques seem feasible and could have a significant impact on the overall plant LCOE. Hybrid concrete/steel towers, as used in wind turbine technology, are promising candidates for this approach.

4. Conclusions

In this study, the cost-saving potential of next-generation CSP plants employing particle technology was assessed. Different variants of these plants were modeled based on the CentRec® receiver technology, a multi-tower approach with a central tubular PHX and one of three steam power cycles (ranging from state of the art to future high-performance developments). These models were then used to simulate, with hourly time steps, the annual electricity yield of each configuration. As a benchmark of state-of-the-art technology, one additional

Table 2
Results of detailed techno-economical comparison of three configurations (*N.B.*: Power block annual efficiency is higher than design point efficiency as the ambient temperature rarely exceeds the design point value of 30 °C.)

Parameter/Result	Unit	Molten salt		Particles			
				540 °C		620 °C	
Parameters (at design point)							
Solar multiple	[–]	3.0		3.2		3.4	
Mirror aperture	[m^2]	1 333 420		1 356 410			
Number of towers	[–]	1		19			
Receiver output	[MW_t]	725.7		770.5			
Receiver aperture area (total)	[m^2]	1359		380			
Tower height (receiver center)	[m]	244.5		90.3			
Optical field efficiency[a]	[%]	63.6		65.3			
Receiver thermal efficiency	[%]	87.8		89.4			
TES capacity	[h]	14		16			
	[MW_th]	3386		3870		3616	
Heat rate PHX in	[MW_t]		241.9			226.0	
TIT	[°C]		540			620	
Power block net efficiency	[%]		41.4			44.4	
Power block net power	[MW_e]			100			
Energy balance annual							
Optical field efficiency	[%]	57.9		55.0			
Receiver thermal efficiency	[%]	85.4		85.2			
Dumping and operating limits efficiency[b]	[%]	91.7		95.6		92.7	
HTM and TES system efficiency	[%]	99.1		97.1		97.1	
Power block net efficiency	[%]	42.5		42.5		45.4	
Plant net efficiency	[%]	41.2		42.2		45.0	
Solar-to-electric efficiency	[%]	18.7		18.3		19.0	
Electricity yield (plant net)	[GW_eh]	628.0		626.3		648.5	
Costs (absolute/fraction of overnight costs)							
Heliostat field	[MEUR]	133.3	(24.7 %)	135.6	(24.5 %)	135.6	(24.2 %
Land	[MEUR]	14.6	(2.7 %)	13.2	(2.4 %)	13.2	(2.4 %)
Receiver	[MEUR]	50.8	(9.4 %)	30.4	(5.5 %)	30.4	(5.4 %)
Towers (excl. TES integration)	[MEUR]	17.2	(3.2 %)	32.4	(5.8 %)	32.4	(5.8 %)
Piping in towers	[MEUR]	0.0[c]	(0.0 %)	6.9	(1.2 %)	7.0	(1.3 %)
Tower transport (vertical)	[MEUR]	0.0	(0.0 %)	6.3	(1.1 %)	6.3	(1.1 %)
Horizontal transport (ground)	[MEUR]	0.0	(0.0 %)	5.9	(1.1 %)	5.7	(1.0 %)
PHX transport (vertical)	[MEUR]	0.0[c]	(0.0 %)	0.6	(0.1 %)	0.6	(0.1 %)
TES tower integration	[MEUR]	0.0[c]	(0.0 %)	8.8	(1.6 %)	8.8	(1.6 %)
TES	[MEUR]	71.1	(13.1 %)	20.8	(3.8 %)	19.7	(3.5 %)
HTM	[MEUR]	0.0[c]	(0.0 %)	24.4	(4.4 %)	22.8	(4.1 %)
PHX	[MEUR]	11.6	(2.1 %)	23.6	(4.3 %)	24.6	(4.4 %)
Balance of plant	[MEUR]	33.9	(6.3 %)	33.9	(6.1 %)	33.7	(6.0 %)
Power block	[MEUR]	78.9	(14.6 %)	78.9	(14.2 %)	86.4	(15.4 %)
EPC indirect & owner's	[MEUR]	129.4	(23.9 %)	132.6	(23.9 %)	134.3	(23.9 %)
Overnight	[MEUR]	540.9	(100.0 %)	554.5	(100.0 %)	561.6	(100.0 %)
O & M	[MEUR/a]	9.5		9.5		9.6	
LCOE	**[EUR-cent/kW_eh]**	**7.11**		**7.28**		**7.12**	

[a]Includes losses due to reflectivity, availability, cosine effect, blocking & shading, attenuation and intercept
[b]Includes losses due to dumping, receiver operating limits and start-up
[c]Included in tower, receiver and TES system cost

model of a single-tower molten salt plant was created. Furthermore, cost models were also set up to evaluate the LCOE for each configuration and optimize the storage capacity as well as the solar field size. Unfortunately, due to the low technological maturity of most particle-related subsystems, their cost correlations had to be derived from estimates or single data points in literature. The main findings from the optimizations and comparisons are the following:

- The lowest LCOE of any particle configuration, under favorable cost assumptions, is approximately equal to the optimized benchmark system (+0.1 %).
- The highest-performance steam process achieves only slightly lower LCOEs than the state-of-the-art process (-2.3 %).
- The techno-economic optima of particle systems are achieved at even larger values for solar multiple and storage capacity than the reference system ($SM > 3.0$ and $Q_{TES,opt} > 14$ h). It is, however, not clear if this suits the demand profile of common applications of CSP plants in the future.
- Compared with the reference plant, savings can mainly be achieved for the receiver and the TES subsystems. However, increased costs for the large number of towers and the PHX more than compensate for the savings.

Finally, several potential improvements to the particle technology were presented and, where possible, an estimate of their potential to improve a plant's techno-economic performance was given. The changes, which are only partially applicable also to molten salt tower systems, include spillage loss utilization, changes to the multi-tower approach, HTM operating temperature optimizations and changes to tower and TES design. While cost estimates for these improvements have a large uncertainty, their combined potential exceeds 15 % in LCOE reduction.

In conclusion, it was shown that the modeled particle technology, even under favorable cost assumptions, does not achieve lower LCOE values than state-of-the-art molten salt tower technology. However, there are areas with high potential of lowering levelized cost, which do not apply to molten salt technology to the same extent. It should, furthermore, be pointed out that other concepts for particle CSP plants exist, for which the qualitative results could look different. This includes systems featuring falling particle receivers (potentially with a higher rating per receiver) or sCO_2 power cycles (which can benefit

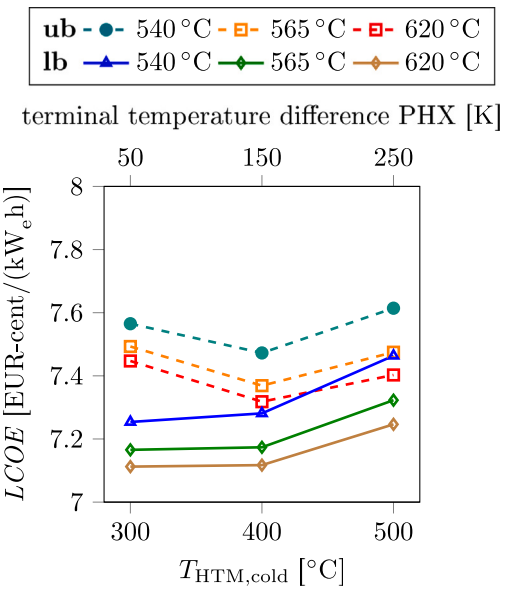

Fig. 9. Sensitivity of LCOE to changes in cold tank temperature, $T_{\mathrm{HTM,cold}}$, for upper and lower bound PHX cost correlations (ub and lb, respectively).

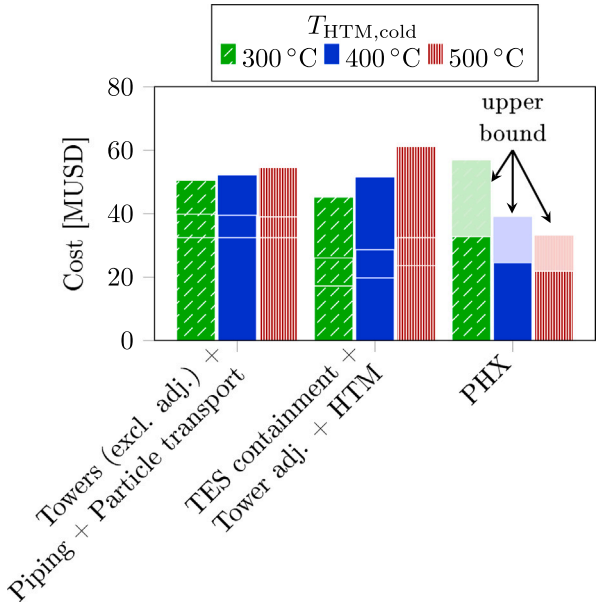

Fig. 10. Effect of changes in cold tank temperature on selected subsystem costs (naming of the stacked bars from bottom to top); light bars represent results acquired using the upper bound cost model; adj.: costs for adjustments in tower structure for TES integration.

from higher operating temperatures than Solar Salt allows for). Although the scope of this study is on electricity generation, solar particle systems also have application potential for high-temperature process heat. In this field, they are able to push the temperatures achievable with direct solar receivers from today 565 °C for molten salt to values beyond 800 °C.

Declaration of competing interest

The authors declare the following financial interests/personal relationships which may be considered as potential competing interests: Dr. Reiner Buck has a part-time affiliation (25 %) with HelioHeat (fully owned by US company Heliogen). HelioHeat is a developer of particle receivers.

Acknowledgments

The authors would like to thank the German Federal Ministry for Economic Affairs and Climate Action for the financial support of the project KOSTPAR (reference number: 0324320).

Appendix A. TES and horizontal transport system costs

The calculation of particle storage and transport system costs is detailed below. The majority of the methodology, as well as the cost assumptions, are based on a joint study by DLR and Sandia National Laboratories [11].

A.1. Particle storage

Two storage tanks (hot and cold) are integrated in the tower one above the other. Cost for reinforcement of the tower structure is included in the tower cost correlation. The inner tower wall forms the outer structure of the tanks, with an assumed tower diameter of 10 m and a container inner diameter (D_{Contain}) of 9.3 m. The height of the containers results from the required particle mass per tower ($m_{\mathrm{HTM,1TES}}$) to achieve the targeted storage capacity, the density of the particle fill (ρ_{HTM}), the temperature difference between hot and cold particles ($T_{\mathrm{HTM,hot}} - T_{\mathrm{HTM,cold}}$), as well as on the effective volume utilization of the fill, VUF [see 11]:

$$m_{\mathrm{HTM,1tower}} = \dot{Q}_{\mathrm{TES,1tower}}/(c_{\mathrm{HTM}} * (T_{\mathrm{HTM,hot}} - T_{\mathrm{HTM,cold}})) \quad (A.1)$$

$$V_{\mathrm{Contain}} = m_{\mathrm{HTM,1tower}}/\rho_{\mathrm{HTM}}/VUF \quad (A.2)$$

$$VUF = 1.11 - 0.000325(T_{\mathrm{HTM,hot}}/°\mathrm{C}) \quad (A.3)$$

$$H_{\mathrm{Contain}} = 4/(\pi D^2_{\mathrm{Contain}}) * V_{\mathrm{Contain}}. \quad (A.4)$$

From these geometric quantities, the insulated surface area can be calculated, which has a large influence on the subsystem costs. Insulation costs for a tank's wall ($C_{\mathrm{Insu,Wall}}$) and ceiling ($C_{\mathrm{Insu,top}}$) were calculated from a specific cost of 1595 USD/m^2, the ceiling costs (C_{Ceil}) themselves assume a thickness of 0.13 m each and a specific costs of 230 EUR/m^3. It was postulated that the cold tank rests on the ground and therefore no further costs are incurred for its floor. The specific costs of the hot tank floor are calculated as

$$c_{\mathrm{Floor,hot}} = 850\,\mathrm{USD/m^2}(0.29 + 2.16 \times 10^{12}(T_{\mathrm{HTM,hot}}/°\mathrm{C})^{-4.6}). \quad (A.5)$$

The two tank floors contain a conical shape of cheaper insulating material, which reduces the dead space and thus the amount of unused particles. The cost per tank is calculated as

$$C_{\mathrm{Flooring}} = 258\,\mathrm{USD} * 0.074(D_{\mathrm{Contain}}/\mathrm{m})^{3.028}. \quad (A.6)$$

The cost of additional pipes and connections for particle transport in the towers was calculated based on the length of the connection, L_{piping},

$$C_{\mathrm{Duct}} = 90\,000\,\mathrm{USD} + 6000\,\mathrm{USD/m} * L_{\mathrm{piping}}. \quad (A.7)$$

The connecting length was assumed to be the difference between the receiver's elevation and the storage system height, H_{st}. Where the latter is derived from tank height, insulation thickness ($s_{\mathrm{iso}} = 1.2$ m), and interstitial spaces ($H_{\mathrm{comp}} = D_{\mathrm{Contain}}$) as follows:

$$H_{\mathrm{st}} = 2(H_{\mathrm{Contain}} + s_{\mathrm{iso}}) + H_{\mathrm{comp}}. \quad (A.8)$$

Particle costs were calculated based on the particle mass for the TES system of one tower, $m_{\mathrm{HTM,1tower}}$, multiplied by a factor of 1.05, which takes into account unused particles in dead spaces of the particle circuit in the overall power plant.

Table B.1
Input parameters for thermodynamic models.

Parameter	Unit	Molten salt	Particles	Comments
Location				
Name	[]		Ouarzazate, Marokko	NoorO complex
Latitude	[°]N		28.298	
Longitude	[°]E		−6.87	
Elevation	[m]		1288	Meteonorm 6.1
Ambient temp. (min./max./mean)	[°C]		−0.3/38.9/18.9	Meteonorm 6.1
Rel. humidity (min./max./mean)	[%]		10/96/38.3	Meteonorm 6.1
Ambient pressure (min./max./mean)	[mbar]		879/898/891	Meteonorm 6.1
Wind speed (min./max./mean)	[m/s]		0.0/13.0/3.3	Meteonorm 6.1, @10 m elevation
Annual DNI	[kWh/(m^{2}a)]		2518	Meteonorm 6.1
Design point				
Design point	[tt : mm − hh]		21.03. – 12:00	
DNI	[W/m^2]		979 (clear sky)	For Design of plant in HFLCAL, clear-sky model is used [18] to calculate the DNI as a function of location, date and time.
Ambient temp.	[°C]		30	Same as power block
Rel. humidity	[%]		60	
Amb. pressure	[mbar]		1013.25	
Wind speed	[m/s]		0	
Atmospheric attenuation: clear	[]		$0.99321 - 1.176 \times 10^{-4} * SLR + 1.97 \times 10^{-8} * SLR^2 @ SLR \leq 1000\,\text{m}$; $e^{-1.106 \times 10^{-4} * SLR} @ SLR > 1000\,\text{m}$	Needed for solar field design in HFLCAL; standard model [24]; SLR: slant range
Heliostats				
Heliostat type	[]		Two-axis, multi facet	Based on Sanlucar 120
Aperture width	[m]		12.93	
Aperture height	[m]		9.57	
Mirrors per heliostat	[–]		28 (4 × 7)	horizontal × vertical
Reflecting area per mirror	[m^2]		4.32	
Optical height (pylon)	[m]		5.02	heliostat center
Reflecting area per heliostat	[m^2]		121	
Reflectivity HFLCAL (annual mean)	[%]		89.34	HFLCAL Input; product of reflectivity (0.94), cleanliness (0.96), availability (0.99)
Beam quality	[mrad]		3.25	HFLCAL Input; combination of slope, tracking and sun shape error
Canting	[]		On-axis	
Power consumption tracking	[kW$_e$]		0	Neglected in annual yield calculation
Solar field				
Number of towers	[–]	1	varied	
Orientation	[]	360°	North	
Tower height above center of receiver	[m]		10	Estimate; needed for shading
Receiver				
Type	[]	Cylindrical, external	Cylindric cavity	
Thermal rating	[MW$_t$]	varied	40.4	|Estimate for commercial system
HTM inlet temp.	[°C]	290	400	[24] |Estimate
HTM outlet temp.	[°C]	565	900	
Receiver model	[]	101	103	HFLCAL models
Absorption	[–]	0.917	0.95	Parameter for receiver models
Emissivity	[–]	0.683	0.9	[24, p. 212] |[10]
Convection heat transfer coeff.	[W/(m^2 K)]	27.7	30	
Reference temp.	[°C]	465.7	900	
Min./max. load	[%]		10/115	Estimate
Particle loss rate	[%/a]		0	Neglected
Elec. consumption	[MW$_e$]	s. HTM	0	|Neglected
Start up time	[min]		20	[24, p. 479]
Heat demand start-up (per tower)	[kW$_t$h]	3630	377	[24, p. 479] |Estimate
Power demand start-up	[kW$_e$h]	3260	0	[24, p. 479] |Neglected
HTM				
Name	[]	Solar Salt	Bauxite	
Heat capacity	[J/(kg K)]	≈1500	1200	[13, p. 148] |[25]
Bulk density	[kg/m^3]	≈1900	2000	[13, p. 148] |[25]
Dyn. viscosity	[mPas]	≈3.5	n.a.	[13, p. 148] |
Vertical HTM transport				
Transport height tower	[m]		105.9	incl. top installations
Pressure increase salt pumps (tower)	[bar]	65.6		based on [13, p. 151] |
Transport height PHX	[m]		30	|Estimate
Pressure increase salt pumps (PHX)	[bar]	4		[24, p. 479] |
Isentr. efficiency salt pumps	[%]	76		[13, p. 151]
Efficiency vert. transport system	[%]		75	|Estimate
Elec. efficiency salt pump motors	[%]	0.97		Estimate |

(*continued on next page*)

Table B.1 (*continued*).

Horizontal HTM transport					
Energy consumption	[MW_e]			0	|Neglected
Thermal losses	[%]			2	|of transp. energy
TES system					
Hot tank temp.	[°C]	565		900	|Neglected
Cold tank temp.	[°C]	290		400	
Heat loss	[%/24 h]		1		|of total capacity
PHX					
Pressure drop, steam	[%]		1		
Heat loss	[%]		0		Neglected
Power block		540 °C	565 °C	620 °C	
Live steam & reheat temp.	[°C]	540	565	620	
Live steam pressure	[bar_a]	140	165	180	
Reheat pressure	[bar_a]	n.a.	23.4	25.2	
Feed water temp.	[°C]		≈250		
Net power	[MW_e]		100		
Net efficiency	[%]	41.35	42.75	44.26	
Ambient temp.	[°C]		30		
Ambient pressure	[$mbar_a$]		1013.25		
Rel. humidity	[%]		60		
Min/Max. load	[%]		25/110		
Cooling	[]		dry		
Generator efficiency	[%]		98.8		
Isentr. efficiency of pumps	[%]		84		
Elec. efficiency motors	[%]		85		

A.2. Horizontal transport system

The cost of the transport system between towers and the central power unit consists of costs for autonomous vehicles (C_{Vehic} = 100 000 USD), for hot and cold transport containers ($C_{\text{Containers}}$ = 90 000 USD + 60 000 USD), as well as loading equipment at each tower ($C_{\text{LoadingEq}}$ = 50 000 USD):

$$C_{\text{TranpH}} = n_{\text{vehic}}(C_{\text{vehic}} + C_{\text{Containers}}) + n_{\text{towers}} C_{\text{LoadingEq}}. \tag{A.9}$$

The number of required vehicles (n_{vehic}) is calculated by dividing the required power plant heat output in nominal operation by the average heat transport capacity of a single vehicle

$$n_{\text{vehic}} = \text{ceil}(\dot{Q}_{\text{PHX,DP}}/\dot{Q}_{1\text{vehic}}). \tag{A.10}$$

The latter can be calculated from the amount of heat transported and the time required for a transport cycle (loading/unloading at the tower, travel time for round trip and loading/unloading at PHX)

$$\dot{Q}_{1\text{vehic}} = E_{\text{container}}/t_{\text{roundtrip}}. \tag{A.11}$$

While the calculation of transported heat quantity per trip is done directly from the estimated loading capacity of 29 823 kg, specific heat capacity, temperature spread of the particles and assumed heat losses ($\eta_{\text{t,transpH}}$ = 98 %):

$$E_{\text{Container}} = \eta_{\text{t,transpH}}\, m_{\text{Pa,1container}}\, c_{\text{HTM}}(T_{\text{HTM,hot}} - T_{\text{HTM,cold}}), \tag{A.12}$$

the average driving distance ($d_{\text{drive,average}}$) and speed ($v_{\text{drive,average}}$) must be specified to determine the driving time

$$t_{\text{roundtrip}} = t_{\text{load,tower}} + t_{\text{load,PHX}} + d_{\text{drive,average}}/v_{\text{drive,average}}. \tag{A.13}$$

The latter was assumed to be 5 m/s and the former calculated via geometric approximations for a power plant composed of equal hexagonal sub-fields which the vehicles drive around:

$$d_{\text{drive,average}} = \left((4.1888 * n_{\text{towers}} - 15.549) L_{\text{side,hexagon}}\right)/n_{\text{towers}} \tag{A.14}$$

$$L_{\text{side,hexagon}} = 2\tan(\pi/6)\sqrt{(A_{\text{land}}/n_{\text{towers}})/\pi}. \tag{A.15}$$

The loading and unloading time per stop ($t_{\text{load,tower}}$ and $t_{\text{load,PHX}}$) was estimated as 10 min each.

Appendix B. Data book

See Table B.1.

References

[1] COMPASsCO2 Project, Development and Testing of New Particles for High-Temperature Concentrating Solar Receivers: state of the Art and Innovation Brought by COMPASsCO2, Informative Paper, 2022, URL https://www.compassco2.eu/wp-content/uploads/2022/04/20220331_InformativePaper1_COMPASsCO2.pdf.

[2] European Commission, HIgh storage density solar power plant for FLEXible energy systems, 2019, URL https://cordis.europa.eu/project/id/857768.

[3] European Commission, Components' and materials' performance for advanced solar supercritical CO2 powerplants, 2020, URL https://cordis.europa.eu/project/id/958418.

[4] European Commission, High temparature concentrated solar thermal power plan with particle receiver and direct thermal storage, 2016, URL https://cordis.europa.eu/project/id/727762.

[5] Solar Energy Technologies Office, Generation 3 concentrating solar power systems (Gen3 CSP) phase 3 project selection, 2022, URL https://www.energy.gov/eere/solar/generation-3-concentrating-solar-power-systems-gen3-csp-phase-3-project-selection.

[6] K.J. Albrecht, M.L. Bauer, C.K. Ho, Parametric analysis of particle CSP system performance and cost to intrinsic particle properties and operating conditions, in: ASME 2019 13th International Conference on Energy Sustainability Collocated with the ASME 2019 Heat Transfer Summer Conference, http://dx.doi.org/10.1115/es2019-3893, Year.

[7] L.F. González-Portillo, K. Albrecht, C.K. Ho, Techno-economic optimization of CSP plants with free-falling particle receivers, Entropy 23 (1) (2021) 76, URL https://www.mdpi.com/1099-4300/23/1/76.

[8] L.F. González-Portillo, K.J. Albrecht, J. Sment, B. Mills, C.K. Ho, Sensitivity analysis of the levelized cost of electricity for a particle-based CSP system, in: ASME 2021 15th International Conference on Energy Sustainability Collocated with the ASME 2021 Heat Transfer Summer Conference, Vol. ASME 2021 15th International Conference on Energy Sustainability, V001T02A008, http://dx.doi.org/10.1115/es2021-63223, Year.

[9] R. Buck, S. Giuliano, Impact of solar tower design parameters on sCO2-based solar tower plants, in: 2nd European SCO2 Conference 2018, 2018, pp. 160–167, http://dx.doi.org/10.17185/duepublico/46098.

[10] R. Buck, S. Giuliano, Solar tower system temperature range optimization for reduced LCOE, AIP Conf. Proc. 2126 (1) (2019) 030010, http://dx.doi.org/10.1063/1.5117522, URL https://aip.scitation.org/doi/abs/10.1063/1.5117522.

[11] R. Buck, J. Sment, Techno-economic analysis of multi-tower solar particle power plants, Sol. Energy 254 (2023) http://dx.doi.org/10.1016/j.solener.2023.02.045.

[12] L. Heller, S. Glos, R. Buck, sCO2 power cycle design without heat source limitations: Solar thermal particle technology in the CARBOSOLA project, in: 4th European SCO2 Conference for Energy Systems, 2021, http://dx.doi.org/10.17185/duepublico/73961.

[13] J. Dersch, J. Paucar, T. Polkas, A. Schweitzer, A. Stryk, Blueprint for Molten Salt CSP Power Plant Final Report of the Project CSP-Reference Power Plant, Report, 2021, URL https://elib.dlr.de/141315/.

[14] Z. Ma, M. Mehos, G. Glatzmaier, B.B. Sakadjian, Development of a concentrating solar power system using fluidized-bed technology for thermal energy conversion and solid particles for thermal energy storage, Energy Procedia 69 (2015) 1349–1359, http://dx.doi.org/10.1016/j.egypro.2015.03.136, URL https://www.sciencedirect.com/science/article/pii/S1876610215004427.

[15] W. Wu, L. Amsbeck, R. Buck, R. Uhlig, R. Ritz-Paal, Proof of concept test of a centrifugal particle receiver, Energy Procedia 49 (2014) 560–568, http://dx.doi.org/10.1016/j.egypro.2014.03.060.

[16] M. Ebert, L. Amsbeck, J. Rheinländer, B. Schlögl-Knothe, S. Schmitz, M. Sibum, R. Uhlig, R. Buck, Operational experience of a centrifugal particle receiver prototype, AIP Conf. Proc. 2126 (1) (2019) 030018, http://dx.doi.org/10.1063/1.5117530, URL https://aip.scitation.org/doi/abs/10.1063/1.5117530.

[17] C. Frantz, R. Buck, L. Amsbeck, Design and cost study of improved scaled-up centrifugal particle receiver based on simulation, J. Energy Resour. Technol. 144 (9) (2022) http://dx.doi.org/10.1115/1.4053784.

[18] P. Schwarzboezl, R. Pitz-Paal, M. Schmitz, Visual HFLCAL - A software tool for layout and optimisation of heliostat fields, in: T. Mancini, R. Pitz-Paal (Eds.), SolarPACES 2009, 2009, URL https://elib.dlr.de/60308/.

[19] T. Baumann, S. Zunft, Development and performance assessment of a moving bed heat exchanger for solar central receiver power plants, Energy Procedia 69 (2015) 748–757, http://dx.doi.org/10.1016/j.egypro.2015.03.085, URL http://www.sciencedirect.com/science/article/pii/S1876610215003914.

[20] R. Buck, G3P3 Techno-Economic Analysis of UpScaled CentRec® Receiver, Report, DLR, 2021, URL https://elib.dlr.de/140177/.

[21] G. Weinrebe, S. Giuliano, R. Buck, A. Macke, A. Burghartz, D. Nieffer, F. Gross, A. Rong, T. Schlichting, K. Blume, HELIKONTURplus - Kostensenkung bei Solarturmkraftwerken durch optimierte Heliostatkonturen plus angepasstes Turm- und Felddesign: Schlussbericht, Report, 2019, http://dx.doi.org/10.2314/KXP:1697318746, URL https://www.tib.eu/de/suchen/id/TIBKAT%3A1697318746.

[22] C.S. Turchi, M. Boyd, D. Kesseli, P. Kurup, M.S. Mehos, T.W. Neises, P. Sharan, M.J. Wagner, T. Wendelin, CSP Systems Analysis - Final Project Report, Report, 2019, http://dx.doi.org/10.2172/1513197, URL https://www.osti.gov/biblio/1513197https://www.osti.gov/servlets/purl/1513197.

[23] Projektträger Jülich, Verbundvorhaben: SpiCoPV - Spillage-Nutzung mit CPV-Modulen, Gesamtkonzept und Solartest, 2021, URL https://www.enargus.de/pub/bscw.cgi/?op=enargus.eps2&q=%2201234198/1%22&v=10&id=5456068.

[24] S. Giuliano, M. Puppe, H. Schenk, T. Hirsch, M. Moser, T. Fichter, J. Kern, F. Trieb, M. Engelhard, S. Hurler, A. Weigand, D. Brakemeier, J. Kretschmann, U. Haller, R. Klingler, C. Breyer, S. Afanasyeva, THERMVOLT : Systemvergleich von solarthermischen und photovoltaischen Kraftwerken für die Versorgungssicherheit, Report, Deutsches Zentrum für Luft- und Raumfahrt e.V. (DLR), Institut für Solarforschung (DLR SF), 2016, http://dx.doi.org/10.2314/GBV:100051305X, URL https://www.tib.eu/de/suchen/id/TIBKAT%3A100051305X/THERMVOLT-Systemvergleich-von-solarthermischen/.

[25] N.P. Siegel, M.D. Gross, R. Coury, The development of direct absorption and storage media for falling particle solar central receivers, J. Sol. Energy Eng. 137 (4) (2015) http://dx.doi.org/10.1115/1.4030069.